High resolution terrain sensing lidar for precision navigation and safe landing of space and aerial vehicles

Farzin Amzajerdian[*a], Aram Gragossian[a], Alexander Bulyshev[b], Paul F. Brewster[a], Jacob M. Heppler[a], Frederick G. Wilson[a], Glenn D. Hines[a], Sean A. Laughter[a], and Daniel K. Litton[a]
[a]NASA Langley Research Center, Hampton, VA 23681, USA; [b]Coherent Applications Inc, Hampton, VA 23681, USA

ABSTRACT

A 3-D imaging flash lidar sensor employing a resolution enhancement algorithm is being developed at NASA Langley Research Center for providing Terrain Relative Navigation and Hazard Avoidance capabilities onboard spacecraft landing on the Moon, Mars, and other planetary bodies. This lidar sensor, we refer to as Terrain Sensing Lidar (TSL), is a solution for future missions that require landing at pre-designated sites near high value resources or at areas of high scientific value, while avoiding hazardous terrain features, such as escarpments, craters, slopes, and rocks, or pre-deployed assets. TSL can also benefit terrestrial applications such as autonomous aerial vehicles without reliance on signals from Global Positioning System (GPS).

The feasibility of the TSL concept has been shown through a series of drone, fixed-wing aircraft, and helicopter flight tests. A prototype version of the TSL has been recently assembled for conducting another set of flight tests to demonstrate its readiness for upcoming landing missions. This paper describes the TSL, provides its performance parameters, and explains its operational concepts for landing missions.

Keywords: 3D Lidar, Flash Lidar, Hazard Detection, Precision Navigation, Terrain Relative Navigation

1. INTRODUCTION

Linear-mode flash lidar offers a viable solution for enabling onboard Hazard Detection and Avoidance (HDA) required by many landing missions including manned and robotic missions to the Moon, Mars, and other planetary bodies.[1,2] The main advantage of flash lidar technology over more conventional scanning lidar is the ability to record full 3-D images with a single laser pulse, freezing the scene on every frame by removing all motion of the transmitter/receiver platform.[3,4] Unlike scanning imaging lidar systems that generate 3-D images by scanning the laser beam across the scene and measuring the time of arrival for each returned laser pulse, a flash lidar records a full 3-D image frame by illuminating the scene with a single laser pulse and imaging the scene onto one Focal Plane Array (FPA). Each pixel in the FPA takes independent measurements of the lidar pulse time of flight to the target. Therefore, the flash lidar does not require position and attitude angle data from external sensors and extensive computation resources and time for compensating vehicle motion during image acquisition. Another advantage is having uniformly distributed pixels within each image frame which simplifies the hazard detection algorithm and reduces the risk of false alarms.[5]

But flash lidars have limited resolution that may be insufficient for many applications. The number of pixels of linear-mode flash lidars is constrained by multiple factors including manufacturing limitations and required laser pulse energy and receiver aperture size for collecting enough returned photons for each pixel to make a range measurement. Current commercially available linear-mode flash lidar focal plane array has 128 x 128 pixels which is grossly insufficient for mapping the designated landing area with the necessary Ground Sample Distance (GSD) for meeting the HDA requirements. Adjusting the Field-Of-View (FOV) of this flash lidar to cover a 100 m x 100 m area will give a GSD of 78 cm (100 m/128), which is much greater than the 15 cm GSD needed for reliably detecting 30 cm radius hazards required by most landing missions. To overcome this shortcoming, past demonstration flight tests used a mechanical gimbal to scan the target area and stitch individual image frames with sufficiently small FOV and GSD.[6] But accommodation of a mechanical gimbal or scanning mirrors on landing vehicles is very challenging or even impractical. For this reason, we employ a novel Super-Resolution (SR) technique[7,8] to eliminate the mechanical gimbal.

[*]f.amzajerdian@nasa.gov; phone 1-757-864-1533.

In SR operation, the lidar FOV is enlarged to cover the whole area of interest and then a sequence of image frames of the same scene, taken from different positions and look angles, are blended to achieve the desired resolution. Our SR algorithm does not require position and attitude (pointing angle) data from an external sensor thus making the flash lidar a standalone instrument. In addition to eliminating the need for a scanning gimbal or mirrors, the SR has several important advantages over stitching individual image frames. The SR technique lowers range measurement noise, recovers bad pixels, and reduces acquisition time (fewer image frames) for generating the desired Digital Elevation Map (DEM). The SR algorithm also provides the six-degree-of-freedom (6-DOF) relative state vector (position and attitude) of the host vehicle with higher precision than most inertial measurements.

We developed a breadboard unit of this lidar, referred to as Terrain Sensing Lidar (TSL), for a series of tests including dynamic testing at NASA LaRC gantry facility, Drone flight tests, and a helicopter flight test. In these tests, the TSL generated high resolution Digital Elevation Maps (DEMs) in real time demonstrating its capabilities for future landing missions.

2. CONCEPT OF OPERATIONS FOR LUNAR LANDING

Another important feature of flash lidar technology is the ability to perform other important functions in addition to the HDA that can help the vehicle to navigate precisely to the designated landing site. A notional operational scenario of the (TSL), is shown in Fig. 1 in the context of a lunar landing. The TSL begins its operation after a deorbit maneuver at about 70 km above the ground. At this stage, the lidar transmitter beam is focused to illuminate only a few pixels, out of 16,384 pixels, in the center of the detector array to measure range to the ground. The lidar has an operational range of 1.4 km when all the detector pixels are illuminated. Reducing the divergence of the lidar transmitter beam to a fraction of its receiver field of view increases its operational slant range to over 70 km from 1.4 km. The ground-relative altitude measurements provided by the TSL reduces the vehicle position error significantly since the Inertial Measurement Unit (IMU) suffers from drastic drift over the travel time from the Earth. The IMU drift error can be about 1 km for a Moon-bound vehicle and 10 km for Mars. Accurate altitude data reduces position error to a few hundred meters.

When the altitude drops to about 20 km, the lidar beam is expanded to illuminate a few hundred detector pixels. In this phase, the TSL generates relatively low-resolution elevation data of the terrain below which are subsequently compared with stored maps of known surface features such as craters. This process, referred to as Terrain Relative Navigation (TRN), further reduces the vehicle's relative position error from hundreds of meters to tens of meters.[9]

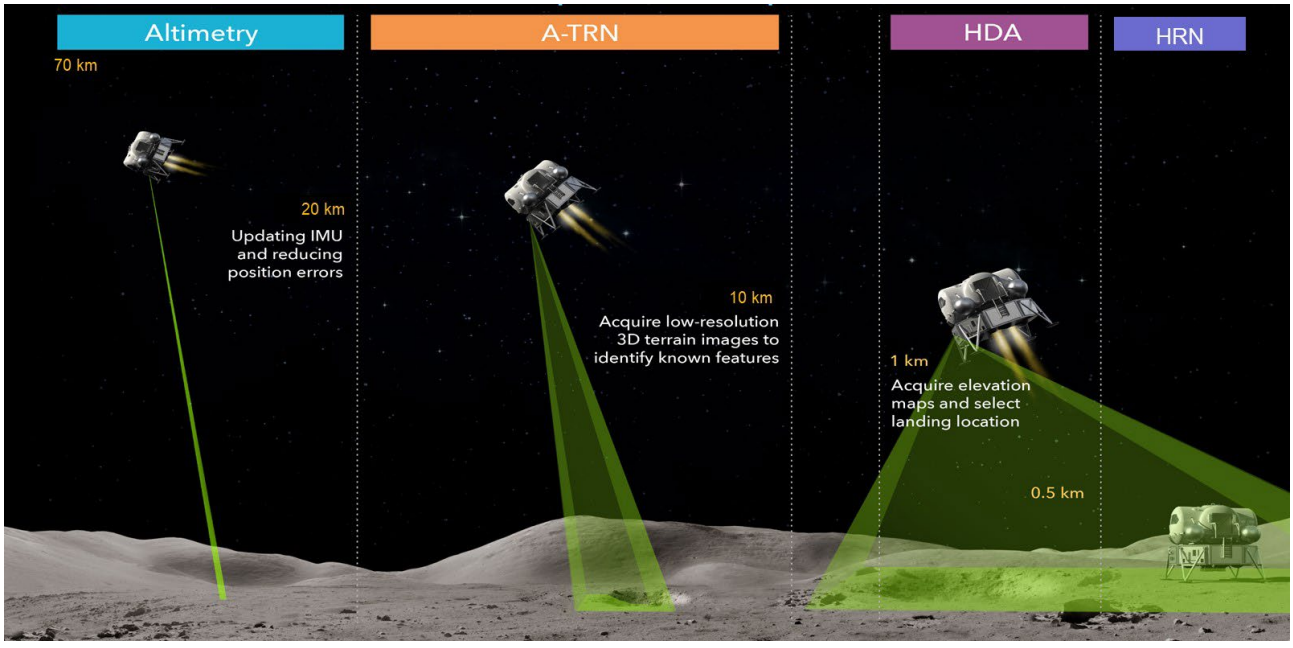

Figure 1. An operational concept of multi-mode Terrain Sensing Lidar (TSL) for lunar landing.

From about 1 km to 0.5 km altitude, the flash lidar operates with its full field of view, generating a high-resolution elevation map of the landing area as described in previous section. This elevation map is then processed to identify hazardous features such as rocks, craters, and steep slopes, and to determine the most suitable landing location (HDA function). Each generated DEM will cover approximately 100 m x 100 m area and can detect hazards greater than 30 cm in radius. As noted earlier, each DEM and the associated hazard maps can be generated in 1 second with a frcation of a a second latency. Therefore, multiple DEMs can be generated in this phase which can be several seconds in duration. These additional DEMs which can be either used for covering a larger area than the specified 100 m x 100 m or for further enhancing the resolution of the DEM and verification of the selected best landing location.

The TSL can continue acquiring range images after selection of the landing location and use the terrain features within the landing site for guiding the vehicle toward the landing location. This phase of the TSL operation is referred to as HRN. The TSL operation terminates at approximately 10 m above the ground before the vehicle thrusters create a dust plume.

3. TSL DEVELOPMENT AND TESTS

We built a breadboard the TSL for conducting a series of ground and airborne tests aimed at characterizing our lidar technique for HDA. This lidar used a linear-mode flash lidar camera, consisting of a focal plane array and associated control electronics, developed by Advanced Scientific Concepts (ASC). The lidar was set to acquire range image frames at 20 Hz for the application of the SR algorithm. The algorithm processed the image frames as they were received by the processer producing high resolution DEMs at 1 Hz rate with about 30 msec latency.

We conducted a set of characterization tests at the NASA LaRC's lidar test range and gantry facilities, followed by a drone flight test.[10] The gantry and drone flight tests allowed for pointing the lidar toward the ground and illuminating all pixels as opposed to horizontal tests pointing to targets of limited sizes that do not completely fill the lidar FOV. Fig. 2 shows the breadboard lidar on the drone flying over calibrated targets placed in a clear area at NASA LaRC.

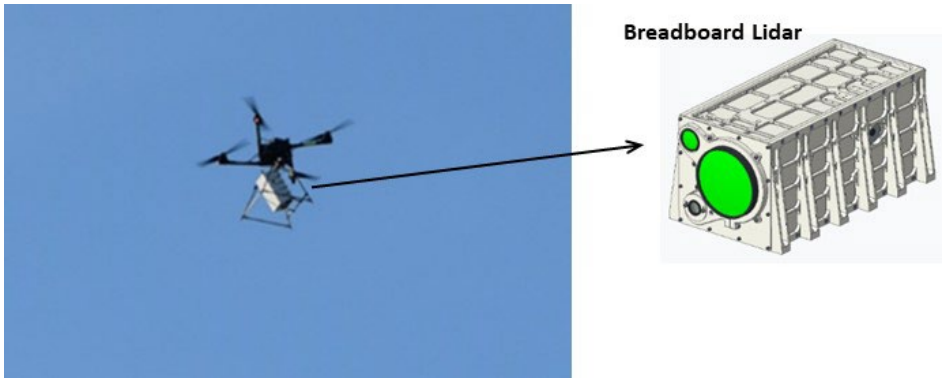

Figure 2. Drone flight test of the breadboard lidar**.**

After completion of the characterization tests, a helicopter flight test campaign was conducted in 2023 at the Blue Origin's Lunar Terrain Field (LTF) in west Texas that was specifically built for testing landing sensors (see Fig. 3). This helicopter flight test allowed for simulating the lunar landing scenarios by flying along different slanted trajectories toward the LTF.

An example of the helicopter flight test data is provided in Fig. 4 showing one of the range image frames that are generated at 20 Hz from about 200 m distance and the corresponding DEM generated 1 Hz. As can be seen, some of smaller rock piles are not resolved in the 3-D range image but clearly detected in the DEM created by the SR algorithm.

Figure 3. A view of the Blue Origin's Lunar Terrain Field with rock piles and craters.

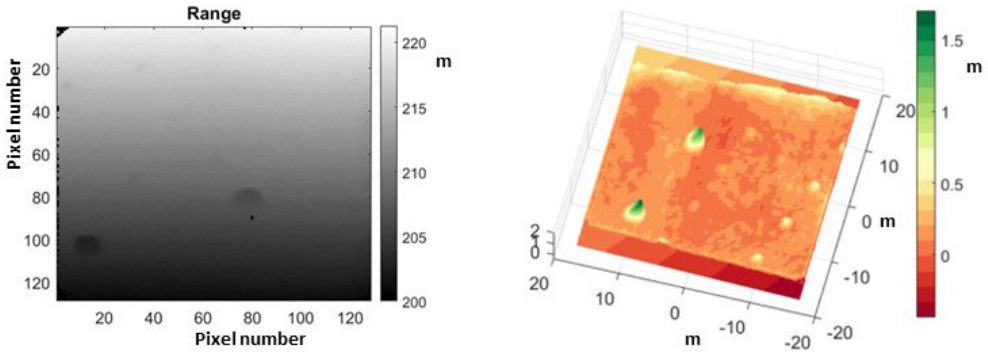

Figure 4. An example of helicopter flight test results, showing a single range image (left) and a high resolution DEM generated in real-time at 1 Hz by applying SR algorithm to 20 consecutive range image frames (right).

Fig. 5 is an illustration of lidar hazard detection performance in which the truth DEM (a) is compared with a lidar-generated DEM (b) by plotting an elevation profile along a line (c) on the generated DEM (b). This data is from about 150 m range at approximately 45 degrees trajectory angle which is representative of most lunar descent trajectories. This elevation profile that includes a small crater and two rock piles shows very good agreement between the truth and the lidar generated DEMs to within a few centimeters, part of which is due to the fact that the truth DEM is not an exact representation of the LTF at the time of the flight test. The truth DEM was generated several years earlier, and the field had experienced significant changes due to weather and natural erosions.

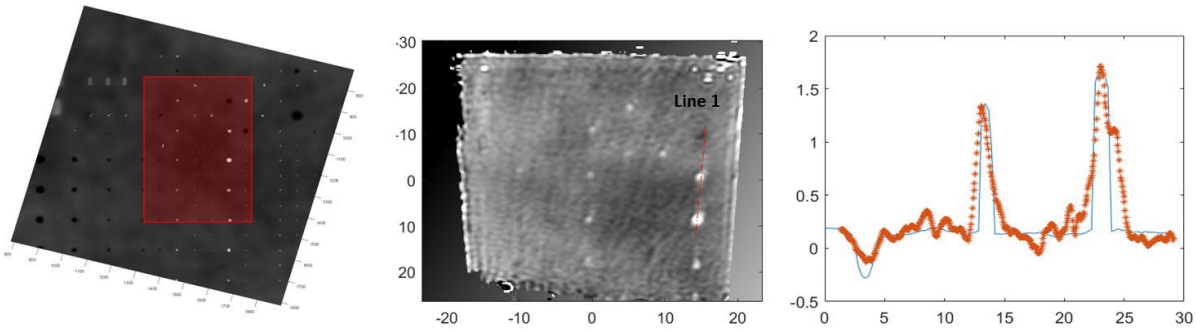

Figure 5. (a) Truth DEM of a section of the LTF, (b) one of the lidar generated DEMs of the highlighted area on the truth DEM, and (c) elevation profile of the lidar DEM along the line 1.

The results of the dynamic tests described above were used for the design and build of a prototype system. The prototype unit includes several upgrades over the breadboard system to extend the HDA operational range to 1400 m, and incorporate multi-mode capability for performing long range altimetry, TRN, and HRN. The prototype system, as shown in Fig. 6, has a compact design with a total mass of 6.5 kg which includes the real-time image processor and command/data interface with the host vehicle.

Figure 6. Terrain Sensing Lidar (TSL) prototype with multi-functional capability.

The TSL prototype is suitable for drone, helicopter, and fixed-wing aircraft flight tests and demonstration of its capabilities for landing missions. These flight tests will help to assess the TSL performance for each of the four functions as described above and serve as a steppingstone for the development of spaceflight units.

TSL can also benefit terrestrial applications such as aircraft navigation without reliance on signals from Global Positioning System (GPS). Conventional aircraft Guidance, Navigation, and Control (GN&C) systems combine Inertial Measurement Unit (IMU) data with GPS signals to determine the vehicle position and velocity vector. GPS position (altitude) data is referenced to sea-level and is of limited value when landing on a moving platform or in limited visibility conditions, or when autonomous navigation and landing is required. Furthermore, GPS signal can be blocked or jammed by intentional or unintentional interference causing significant deviation in the navigation solution. TSL, operating as a standalone sensor, provides precise terrain-relative position and velocity data.

CONCLUSION

A lidar sensor based on linear-mode flash lidar technology and by utilizing a novel Super-Resolution algorithm is being developed to meet the needs of future landing missions requiring precision safe landing at designated locations on the Moon or other destinations in the solar system. This multi-functional lidar sensor, referred to as Terrain Sensing Lidar (TSL) can enable long distance altimetry, Terrain Relative Navigation, Hazard Detection and Avoidance, and Hazard Relative Navigation. The merits of the TSL have been demonstrated by a series of static and dynamic tests of a breadboard unit including drone and helicopter flight tests. The results of these tests led to the development of a compact and robust prototype system for further flight testing, including high altitude flights, that can pave the path for the development of spaceflight units. The TSL can also benefit terrestrial aerial vehicles requiring autonomous operation in GPS-denied environment.

ACKNOWLEDGMENTS

The authors are grateful to the Center Director's Office and the Space Technology and Exploration Directorate at NASA Langley Research Center for their continued support. The authors also acknowledge Blue Origin for facilitating the helicopter flight test campaign.

REFERENCES

[1] Epp, C. D., Robinson, E. A., and Brady, T., "Autonomous Landing and Hazard Avoidance Technology (ALHAT)", Proc. of IEEE Aerospace Conference, paper no. 1644, 2008.

[2] Carson III, J. M., Robertson, E. A., Trawny, N., and Amzajerdian, F., "Flight Testing ALHAT Precision Landing Technologies Integrated Onboard the Morpheus Rocket Vehicle," Proc. AIAA Space 2015 Conference & Exposition, Pasadena, CA, 2015.

[3] Farzin Amzajerdian, Vincent E. Roback, Alexander E. Bulyshev, Paul F. Brewster, William A. Carrion, Diego F. Pierrottet, Glenn D. Hines, Larry B. Petway, Bruce W. Barnes, and Anna M. Noe, "Imaging flash lidar for safe landing on solar system bodies and spacecraft rendezvous and docking," Proc. SPIE Vol 9465, 2015.

[4] Farzin Amzajerdian, Vincent E. Roback, Alexander Bulyshev, Paul F. Brewster, Glenn D. Hines, "Imaging Flash Lidar for Autonomous Safe Landing and Spacecraft Proximity Operation," AIAA SPACE Forum, (AIAA 2016-5591) 10.2514/6.2016-5591, 2016.

[5] Alexander Bulyshev and Farzin Amzajerdian, "Hazard Avoidance Algorithm for a 3-D Imaging Flash Lidar Utilizing Multi-Frame Super-Resolution Technique," AIAA Guidance, Navigation, and Control Conference, AIAA SciTech Forum, 2023.

[6] Vincent E. Roback , Diego F. Pierrottet, Farzin Amzajerdian, Bruce W. Barnes, Glenn D. Hines, Larry B. Petway, Paul F. Brewster, Kevin S. Kempton, and Alexander E. Bulyshev, "Lidar sensor performance in closed-loop flight testing of the Morpheus rocket-propelled lander to a lunar-like hazard field," Proc. of AIAA Science and Technology Forum and Exposition, 2015.

[7] A. Bulyshev, F. Amzajerdian, V. E. Roback, G. Hines, D. Pierrottet, and R. Reisse, "Three-dimensional super-resolution: theory, modeling, and field test results," Appl. Opt. 53(12), 2583, 2014.

[8] Alexander Bulyshev, Farzin Amzajerdian, Eric Roback, Robert Reisse, "A super-resolution algorithm for enhancement of flash lidar data: flight test results," Proc. SPIE Vol. 9020, 2014.

[9] Johnson, A.E., and Montgomery, J., "An Overview of Terrain Relative Navigation for Precise Lunar Landing," IEEE Aerospace Conference, 2008.

[10] Farzin Amzajerdian, Paul Brewster, Alexander Bulyshev, Aram Gragossian, Jacob M. Heppler, Glenn D. Hines, Daniel K. Litton, Frederick G. Wilson and Sean Laughter, "Multi-functional flash lidar for precision safe landing in challenging terrains," Proc. of AIAA Science and Technology Forum and Exposition, 2024.